

Inhibition of Dormant Lung Cancer Cell Reactivation by *Punica Granatum Peel* and *Dioscorea Nipponica*: Involving MYC, SKP2 and p27

Su Su Thae Hnit^{1,*}, Ling Bi^{2,*}, Chanlu Xie¹, Ling Xu³, Yi Zhong⁴, Ming Yang⁵, Yan Wang^{2,6}, Qihan Dong¹

¹Sydney Chinese Medicine Anti-Cancer Evaluation Pty, Sydney, NSW, Australia; ²Department of Oncology, Shuguang Hospital, Shanghai University of Traditional Chinese Medicine, Shanghai, People's Republic of China; ³Department of Oncology, Yueyang Hospital of Integrated Traditional Chinese and Western Medicine, Shanghai University of Traditional Chinese Medicine, Shanghai, People's Republic of China; ⁴Department of Oncology, Shanghai Hospital of Integrated Traditional Chinese and Western Medicine, Shanghai University of Traditional Chinese Medicine, Shanghai, People's Republic of China; ⁵Department of Pharmacy, Longhua Hospital, Shanghai University of Traditional Chinese Medicine, Shanghai, People's Republic of China; ⁶The Second Clinical Medical College of Guizhou University of Traditional Chinese Medicine, Guizhou Province, People's Republic of China

*These authors contributed equally to this work

Correspondence: Qihan Dong; Yan Wang, Email qihan.dong@mq.edu.au; yanwang@shutcm.edu.cn

Introduction: Dormant cancer cells, capable of reactivating from the G₀ phase, drive tumor recurrence and therapy resistance. Current clinical strategies targeting dormancy remain limited. This study evaluates *Punica granatum peel* (PGP) and *Dioscorea Nipponica* (DN) for their ability to sustain dormancy in lung cancer cells and inhibit reactivation.

Methods: Dormancy was induced in A549 and H460 lung cancer cells via contact inhibition or serum deprivation. Subcutaneous and orthotopic xenograft mouse models were employed. Cells and mice were treated with PGP, DN, or their combination. SYBR Green assays, flow cytometry, and immunoblotting assessed DNA synthesis, cell cycle phases, and protein expression (p27, SKP2, cMYC, AURORA A, SUPT16H, SSRP1).

Results: Both PGP and DN significantly inhibited DNA synthesis and cell cycle re-entry (G₀-to-G₁ transition) in vitro. In vivo, tumor volume and weight decreased by 26–50% (p < 0.05) in treated mice. Treatments upregulated p27 while downregulating SKP2, cMYC, AURORA A, SUPT16H, and SSRP1. No synergistic effect was observed, but additive efficacy (Combination Index ≈ 1) was noted at a 10:1 PGP:DN ratio.

Discussion: PGP and DN sustain dormancy by modulating key cell cycle regulators, highlighting their potential to reduce recurrence and combat drug resistance. These findings underscore the therapeutic promise of traditional Chinese medicines in managing dormant cancer cells. Future studies should identify active compounds and validate mechanisms in advanced models.

Keywords: lung cancer, dormant cancer cells, *Punica granatum peel*, *Dioscorea nipponica*, SSRP1, MYC and SKP2

Introduction

Lung cancer persists as the predominant cause of cancer-related deaths globally. In 2020, it was responsible for 2.2 million new cases and 1.8 million deaths worldwide, affecting both men and women.¹ Notably, the mortality from lung cancer in the United States surpasses the combined fatalities from breast, prostate, and colon cancers.² Advances in low-dose spiral computed tomography (CT) scanning have improved early-stage detection and increased the eligibility for surgical interventions. Despite these advances, the rate of postoperative recurrence remains high and continues to drive mortality rates. Patients diagnosed at advanced stages often face prognoses too severe for curative surgery. Moreover, the emergence of resistance to third-generation targeted therapies and immunotherapies poses significant challenges to effective treatment.^{3,4}

Recent advances in understanding the molecular and cellular mechanisms of tumor recurrence and drug resistance have highlighted the critical role of tumor cell dormancy.^{5,6} Dormant tumor cells can temporarily halt proliferation, surviving



treatments aimed at actively dividing cells, and can later reactivate, leading to recurrence and resistance. This knowledge has spurred the investigation of various strategies to manage dormant tumour cells, including maintaining their dormancy, sensitizing them to anti-cancer drugs, or eradicating them entirely.⁷ Among the strategies explored, estrogen receptor modulators^{8,9} and CDK4/6 inhibitors¹⁰ primarily focus on blocking cell cycle re-entry through inhibition of single molecular target.

This study introduces a novel strategy using Punica granatum peel (PGP) from *Punica granatum L.* and Dioscorea Nipponica (DN) from *Dioscorea nipponica* Makino, two traditional Chinese medicines (TCMs) that target multiple molecular regulators of dormancy. PGP, rich in bioactive polyphenols such as punicalagin and ellagic acid, has demonstrated broad antitumor effects, including induction of apoptosis, inhibition of proliferation, and suppression of metastatic pathways in breast,^{11,12} prostate,^{13,14} and colon cancers.^{12,15} Notably, PGP extracts modulate cell cycle regulators like cyclins and CDKs, suggesting inherent potential to influence dormancy dynamics.¹⁶ Similarly, DN, a source of steroidal saponins (eg, dioscin and gracillin), exhibits antitumor activity by disrupting mitochondrial function, promoting ROS-mediated apoptosis, and inhibiting epithelial-mesenchymal transition in lung¹⁷ and hepatic cancers.^{18–21} Its ability to downregulate MYC and SKP2 in prior studies aligns with our focus on dormancy-related pathways.^{22,23} Our study demonstrates that, unlike conventional single-target therapies, PGP and DN exhibit a unique polypharmacological mechanism: they stabilize the dormancy-enforcing protein p27 while concurrently suppressing reactivation drivers including SKP2 and cMYC. This dual-action, multi-target approach addresses the multifactorial nature of dormancy. Furthermore, the natural origin and preclinical safety profile offer a potential therapeutic advantage over single target synthetic inhibitors.

Materials and Methods

Preparation of Agents for Treatment

Punica granatum peel (PGP) and Dioscorea Nipponica (DN), derived from *Punica granatum L.* and *Dioscorea nipponica* Makino, respectively, were procured as dried water extract granules from Jiangyin Tianjiang Pharmaceutical (<https://www.tianjiangus.com/>). The batch numbers were #20040131 for PGP and #20051413 for DN, authentication by Chinese Pharmacopoeia. The dried granules were dissolved at 200 mg/mL in a 1:1 (v/v) mixture of DMSO and milliQ water to prepare the stock solution and stored at 4°C.

Dormancy and Reactivation Model in vitro

Lung cancer cell lines A549 (CCL-185) and H460 (HTB-177) were sourced from American Type Culture Collection (ATCC) and cultured in RPMI 1640 medium, supplemented with 10% v/v foetal bovine serum (FBS; AusGeneX, Brisbane, QLD, Australia), 100 U/mL penicillin and 100 µg/mL streptomycin, at 37°C with 5% CO₂ atmosphere. A549 cells reached dormancy at 100% confluence maintained for 3 days, while H460 cells were grown to 70–80% confluence, then subjected serum deprivation for 5 days to induce dormancy. Cell cycle reactivation was triggered by diluting A549 cells 1:10 or replating H460 cells in serum-containing medium.

Retroviral Transduction

pMXs-IP-mVenus-p27K⁻ was provided by Dr Toshihiko Oki (The University of Tokyo, Japan). The constructs were mixed with packaging plasmids,²⁴ transfected into 50% confluent HEK293T cells using a calcium phosphate precipitation. The lentiviral particles were then used to infect A549 and H460 cells in the presence of 8 µg/mL polybrene. Infected cells with mVenus-p27K⁻ construct were selected with 0.2 mg/mL puromycin²⁵ and further cultured to isolate single-cell colonies expressing mVenus for subsequent experiments.

SYBR Green Assay

For experimental re-entry model, A549 and H460 (5000 cells/well) were seeded in 96-well plates and treated with PGP, DN, or their combination to achieve the indicated dose for 3 days. H460 cells (10,000 cells/well) were seeded in serum-free culture medium for 5 days followed by 3 days period of treatment in serum-free culture medium. For SYBR green assay as described,²⁵ duplicates of cells/well before treatment were stored at –80°C and used as a baseline representing

the DNA content at the time zero of treatment. The cells were then harvested, and the fluorescence intensity (FI) of DNA content of both baseline and treated cells was measured. The growth inhibition (GI) was calculated as described.²⁶

Determination of Combination Ratio in vitro

The ratio between PGP and DN in vitro was assessed using CalcuSyn software (Biosoft, Cambridge, UK). The combination index (CI) value was derived from the dose–effect relationships of both drugs, individually and in combination, according to the Chou-Talalay method. The dose–effect curves were constructed using data obtained from SYBR Green assays, where varying concentrations of PGP and DN were applied to the target cells. Data analysis through CalcuSyn software involved inputting the dose and corresponding effect levels for each drug alone and in combination. Common thresholds are $CI < 1$ for synergy, $CI = 1$ for additivity, and $CI > 1$ for antagonism.

Flow Cytometry

Cell cycle analysis was performed on A549 and H460 cells (4×10^5 and 5×10^5 cells respectively) treated with PGP, DN, or their combination for 24 hours, followed by trypsinization and fixation in 70% ethanol at 4°C overnight. The cellular DNA was labeled with Hoechst 33342 (H21492, Molecular Probes) at 4 µg/mL at 37°C in dark for 45 min followed by incubation with Pyronin Y (18614, Polysciences) at 8 µg/mL at room temperature in dark for further 15 min to label cellular RNA. The stained cells were analysed using a Gallios flow cytometer (Beckman Coulter Life Science) with FlowJo software for data analysis, as described previously.^{14,25}

Immunoblotting

Treated A549 and H460 cells were lysed with RIPA buffer containing protease and phosphatase inhibitors (11836145001; Roche) and 50 mm sodium fluoride (S7920, Sigma-Aldrich), sonicated, and centrifuged to collect supernatants for immunoblotting, as described previously.²⁷ Proteins were separated by SDS-PAGE, transferred to PVDF membranes, and probed with antibodies. The primary antibodies against SKP2 (2652), c-MYC (13987), SUPT16H (12191) and SSRP1 (13421) were purchased from Cell Signaling Technology, and antibodies against p27 (sc-528), and α -tubulin (SC-5286) were from Santa Cruz Biotechnology. Detection was performed using enhanced chemiluminescence (ECL) and captured on a ChemiDoc MP imaging system (Bio-Rad).

In vitro Digestion Test

This test was conducted to evaluate the stability of PGP and DN under simulated gastric and intestinal conditions, following the method²⁸ with some modification. 100 mg of PGP, DN and combination was dissolved in milli Q water at 20 mg/mL. 1 mL of dissolved solution was kept as control and the remaining solution was adjusted to pH 2 with HCl followed by incubation with 5 mg/sample of pepsin from porcine stomach mucosa (P6887, Sigma-Aldrich) for 2 hours in a shaking bath. Samples were then neutralized with NaHCO₃ to pH 8.0 and incubated with 20 mg/sample of pancreatin from porcine pancreas (193975, MP Biomedicals) and 200 µg/mL of bile extract mixture (B8756, Sigma-Aldrich) for 2 hours in a shaking bath. The samples were then adjusted to pH 7.4 using RPMI 1640 culture medium to obtain a total of 20 mL. To stop the activity of digestive enzymes, both control and enzymes treated samples were heated for 15 minutes at 95°C. The samples were then filtered with 0.22 µm filter (SLGP033RS, Millipore) and diluted with culture medium for the desired treatment concentration.

Human Lung Cancer Xenograft Model in Mice

H460 (1×10^7 cells in 0.2 mL of PBS) was inoculated subcutaneously into the left flank of 7-week-old BALB/c nude mouse. When tumour formed in 3–4 weeks in the size of a soybean, tumours were removed and cut into 2 mm³. Each piece was then implanted through a puncture needle into individual mouse followed by randomly assigning into the control and treatment groups (n = 8 per group). In the next day, PGP or DN was dissolved in normal saline, vortex and preheat at 37°C water baths for 30 min before given via oral gavage. The human daily dose of PGP is 9 g, and DN 15 g, based on the Chinese Pharmacopoeia.²⁹ The ratio of PGP and DN to dried powder of water extracts was 5:1 and 6:1, respectively (w/w). Based on twice the human daily dose and the conversion coefficient of 0.0026 for 20 g mice, 9.4 mg

of PGP or 13 mg of DN in 0.2 mL of normal saline was given to each mouse daily. For the control group, 0.2 mL of normal saline was given by gavage. The H460 xenograft was monitored by calibre measurement and tumour volume was calculated as $\text{volume} = (\text{length} \times \text{width}^2)/2$. The study was approved by Institutional Animal Care and Use Committee (IACUC) of Shanghai Model Organisms Centre (Approval number #2019-0011).

Human Lung Cancer in situ Model in Mice

Female BALB/c nu/nu mice, 4-week-old, were used for lung orthotopic tumour implantation. 5×10^6 H460-luc cells in 50 μL of HBSS were injected into the point of intersection of the horizontal line along the xiphoid to the right chest and the vertical line from the right axillary down. D-Luciferin (150 mg/kg) was injected intraperitoneally ~7 mins before detection, tumour burden signal was detected by IVIS spectrum xenogen machine (Caliper Life Sciences). On day 10 post-injection, mice were randomly assigned to control, PGP, DN and the combination group ($n = 8$ per group). The dose range and administration of the treatment were the same as in the xenograft model. Bioluminescence analysis was performed using Living Image software. The study was approved by Institutional Animal Care and Use Committee (IACUC) of Shanghai Model Organisms Centre (Approval number #2019-0011). All animal procedures are strictly complied with the Guideline for the Welfare and Ethical Review of Laboratory Animals (35892–2018), which is the national standard issued by the Standardization Administration of China (SAC). This guideline governs ethical review, housing conditions, and humane endpoints for the use of laboratory animals in China.

Chemical Profiling of PGP and DN Using LC MS/MS

Ultra-High Performance Liquid Chromatography coupled with Quadrupole Time-of-Flight Mass Spectrometry (UPLC-Q-TOF-MS) was employed to identify chemical constituents within the PGP and DN samples. Sample preparation involved grinding the PGP (2g) or DN (1g) granules into a fine powder, added to a 50 mL conical flask with 20 and 10 mL of 50% methanol, respectively. The mixture underwent ultrasonication at 300 W and 40 kHz for 30 minutes, was then cooled, shaken, and centrifuged at 12,000 rpm for 5 minutes to obtain the supernatant. The analysis utilized a Waters ACQUITY UPLC HSS T3 column (2.1×100 mm, $1.8 \mu\text{m}$) with a column temperature maintained at 30°C and a flow rate of 0.3 mL/min. The mobile phase consisted of acetonitrile (A) and 0.1% formic acid in water (B). For Mass Spectrometric analysis, the AB Sciex Triple TOF[®] 4600 system was used in both negative and positive ion modes. The TOF mass range was set from 50 to 1700 m/z.

Statistical Analysis

SPSS (version 29) and GraphPad Prism 9.2.0 were used for data analysis. Normality of data distributions was confirmed using the Shapiro–Wilk test prior to ANOVA. For comparisons between individual groups where sample sizes were larger, Fisher's LSD multiple comparison test was applied, and differences were considered statistically significant at $p < 0.05$. For analyses involving smaller sample sizes (eg, cell-phase data with $n = 5$ per group), recommended stratified bootstrapping with 5000 resamples was performed to calculate bias-corrected and accelerated (BCa) 95% confidence intervals for multiple comparisons.³⁰ Statistically significant differences were determined when the confidence intervals excluded zero.

Results

Inhibition of DNA Synthesis by PGP and DN in Reactivated Lung Cancer Cells

The re-entry of dormant cancer cells into the cell cycle is marked by the resumption of DNA synthesis. Thus, we investigated the effect of Punica granatum peel (PGP) and Dioscorea Nipponica (DN) on DNA synthesis in lung cancer cells transitioning from a dormant state. Dormancy in A549 and H460 cells was induced by contact inhibition and serum deprivation, respectively. Reactivation was achieved either by dilution of contact inhibited cells or reexposure to serum. Upon reactivation from dormancy, cells were treated with PGP, DN, or their combination. All three treatments exhibited a dose-dependent inhibition of DNA synthesis at 48 h and 72 h post-dormancy in both cell lines (Figure 1a). The half-maximal inhibitory concentration (GI_{50}) from each treatment at 72 h is presented in [Supplementary Table 1](#). The combination efficacy of PGP and

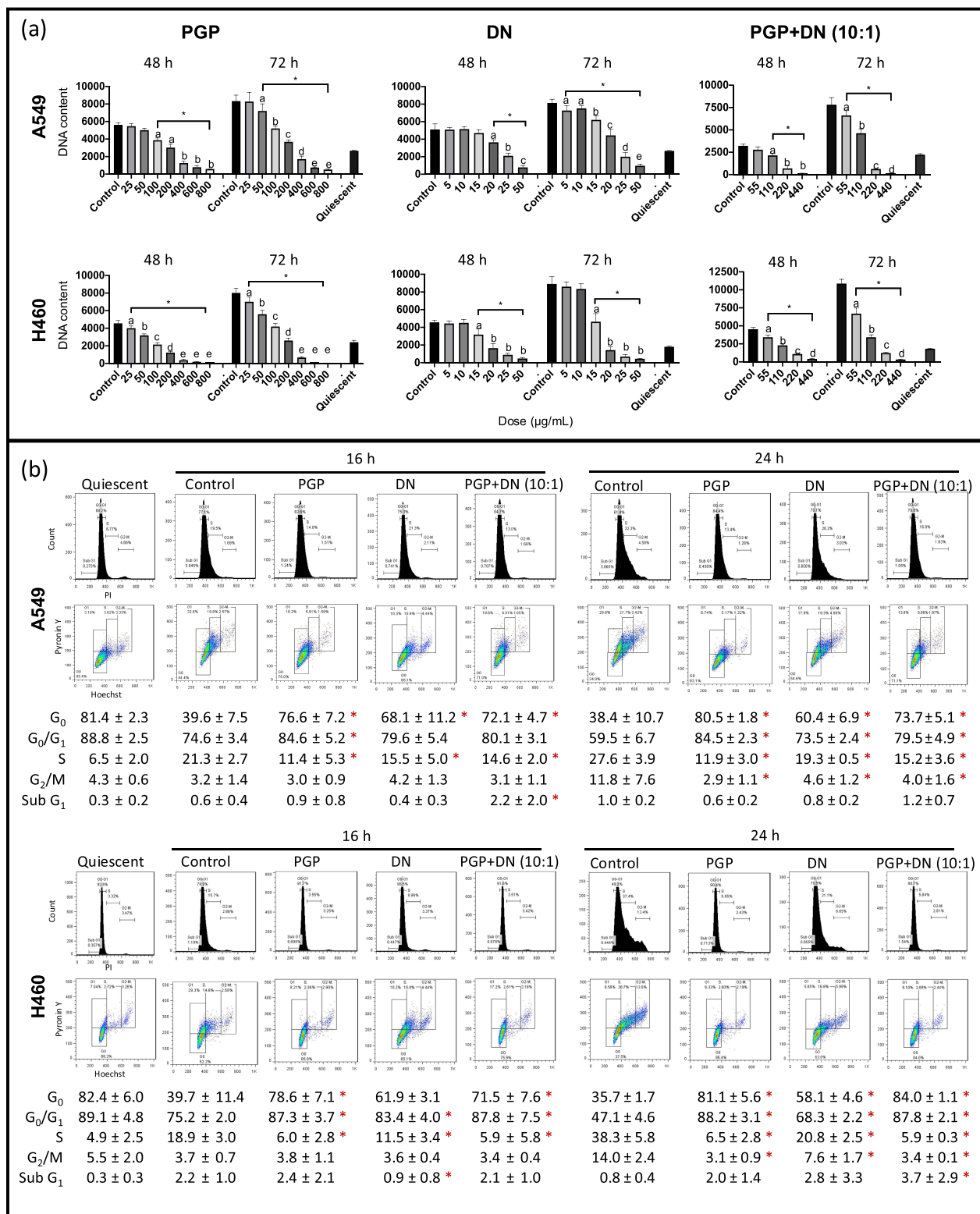


Figure 1 Inhibition of cell cycle re-entry by PGP, DN, and their combination in lung cancer cells. **(a)** Lung cancer cells were synchronised at the G_0 state, and various dose ranges of PGP, DN and the combination were introduced upon cell cycle re-entry. Cells were harvested at 48 h and 72 h of cell cycle re-entry, and DNA content was analysed using SYBR Green assay. Data expressed as mean ± SD (n = 6) of DNA content; * indicates statistical significance compared with the control (p < 0.05) and different letters (a, b, c, d, e) indicate statistical significance among the doses (p < 0.05). **(b)** Treating lung cancer cells upon cell cycle re-entry with PGP, DN and the combination, and cells were harvested at 16 h and 24 h for cell cycle analysis by flow cytometry. Representative histograms of Hoechst staining alone and dot plots of co-staining of Hoechst and Pyronin Y were presented. Data expressed as mean ± SD (n = 4). * indicates statistically significant differences when the confidence interval between the treated groups and control exclude zero.

DN was analyzed using CalcuSyn software. Although no synergistic effect ($CI < 1$) was observed in the tested dose range in both cell lines, a ratio of 10–20:1 (PGP:DN) had a CI value close to 1 whereas a significantly high CI was noted at a 1–5:1 ratio ([Supplementary Table 2](#)). Since no statistical difference was present between the 10:1 and 20:1 ratios at ED_{50} , consequently, a 10:1 ratio was selected for treatments of both cell lines.

Cell Cycle Arrest from G_0 to G_1 by PGP and DN

Then, we examined the distribution of cell cycle phases to ascertain how these treatments suppressed DNA synthesis. Dormant A549 and H460 cells were reactivated and treated with PGP (400 $\mu\text{g}/\text{mL}$), DN (40 $\mu\text{g}/\text{mL}$), or their combination (400 $\mu\text{g}/\text{mL}$ PGP + 40 $\mu\text{g}/\text{mL}$ DN). The treated cells were harvested at 16- and 24 h post-dormancy release, followed by Hoechst 33342 staining for cell cycle analysis. To assess the transition from G_0 to G_1 phase specifically, we employed a dual staining approach using Hoechst 33342 and Pyronin Y, leveraging the lower RNA content characteristic of the G_0 phase.³¹ Vehicle-treated control cells exhibited a decrease in the G_0 fraction at both 16 h and 24 h post-dormancy, compared with dormant cells, indicative of cell cycle reactivation. In contrast, treatment with PGP, DN or their combination inhibited this transition, maintaining a significant proportion of cells in the G_0 phase ([Figure 1b](#)). For both 16 h and 24 h, all treatments had effectively reduced the population of cells progressing into the DNA synthesis phase.

Modulation of Proteins Maintaining or Awakening Dormancy by PGP and DN

To elucidate the effects of PGP and DN on cell cycle re-entry mechanisms, we utilized A549 and H460 cells transfected with mVenus-p27K⁻ plasmids. These treatments were applied upon reactivation from the dormant state, with cellular imaging conducted at dormancy, and 24 h and 48 h post-release. Control cells exhibited a notable decrease in mVenus-p27K⁻ levels 24 h after dormancy release. Conversely, treatment with PGP, DN, or their combination maintained, to large extent, levels of mVenus-p27K⁻, suggesting an inhibition of cell cycle reactivation ([Figure 2a and b](#)).

Further analysis focused on the p27 signaling network, crucial for cell cycle progression. We assessed the expression of proteins that either promote or inhibit cell cycle re-entry, specifically cMYC, AURORA A, SKP2 (all re-entry promoters), and p27 (re-entry inhibitor) following 24 h post-dormancy. Results demonstrated that all three treatments effectively down-regulated cMYC, AURORA A, and SKP2, while up-regulating p27 levels ([Figure 3a and b](#)). Moreover, PGP alone and in combination with DN reduced SUPT16H and SSRP1 levels, with DN alone prominently decreasing SUPT16H levels.

The expression levels of the key regulators in human cancer tissues were examined using the TCGA database. AURORA A, SKP2, SSRP1, and SUPT16H were aberrantly elevated at mRNA levels in lung adenocarcinoma compared with either same individual adjacent (paired) or other individual (unpaired) normal tissues ([Figure 3c and d](#)).

Efficacy of Oral Administration of PGP and DN in Xenograft Models

An *in vitro* digestion test was performed to evaluate the stability of PGP and DN against gastrointestinal enzymes, with their impact on DNA content assessed via SYBR Green DNA analysis ([Supplementary Figure 1](#)). The results indicated that the anti-cancer properties were stable and not degraded by pepsin or pancreatin, supporting their suitability for oral administration.

In vivo efficacy was assessed using a subcutaneous H460 cell xenograft model in mice. Starting on the second day post-implantation, mice were orally administered 9.4 mg of PGP or 13 mg of DN dissolved in 0.2 mL of normal saline, while the control group received 0.2 mL of normal saline alone. Significant tumor volume reductions were observed in the treated groups from Day 16 for PGP and Day 11 for DN, with reductions of 26% and 50% in tumor size, respectively, by the end of the study ([Figure 4a](#)). Tumor weight decreased by 36% in the PGP group and 50% in the DN group, with statistical significance ($p < 0.03$, [Figure 4b](#)). The body weight of the animals remained stable throughout the experiment ([Figure 4c](#)).

Additionally, H460-luc cells were used to establish an orthotopic lung cancer model with tumors localized via transthoracic injections. After 8 days, treatments were administered at the same (High dose) and half of (Low dose) dosages used in the subcutaneous model. Tumor progression was monitored weekly by bioluminescence imaging. On day 30 post-injection, a significant reduction in tumor burden by 63% was noted across all High dose treatment groups compared to controls ($p < 0.05$, [Figure 4d and e](#)), without affecting the overall body weight of the mice ([Figure 4f](#)).

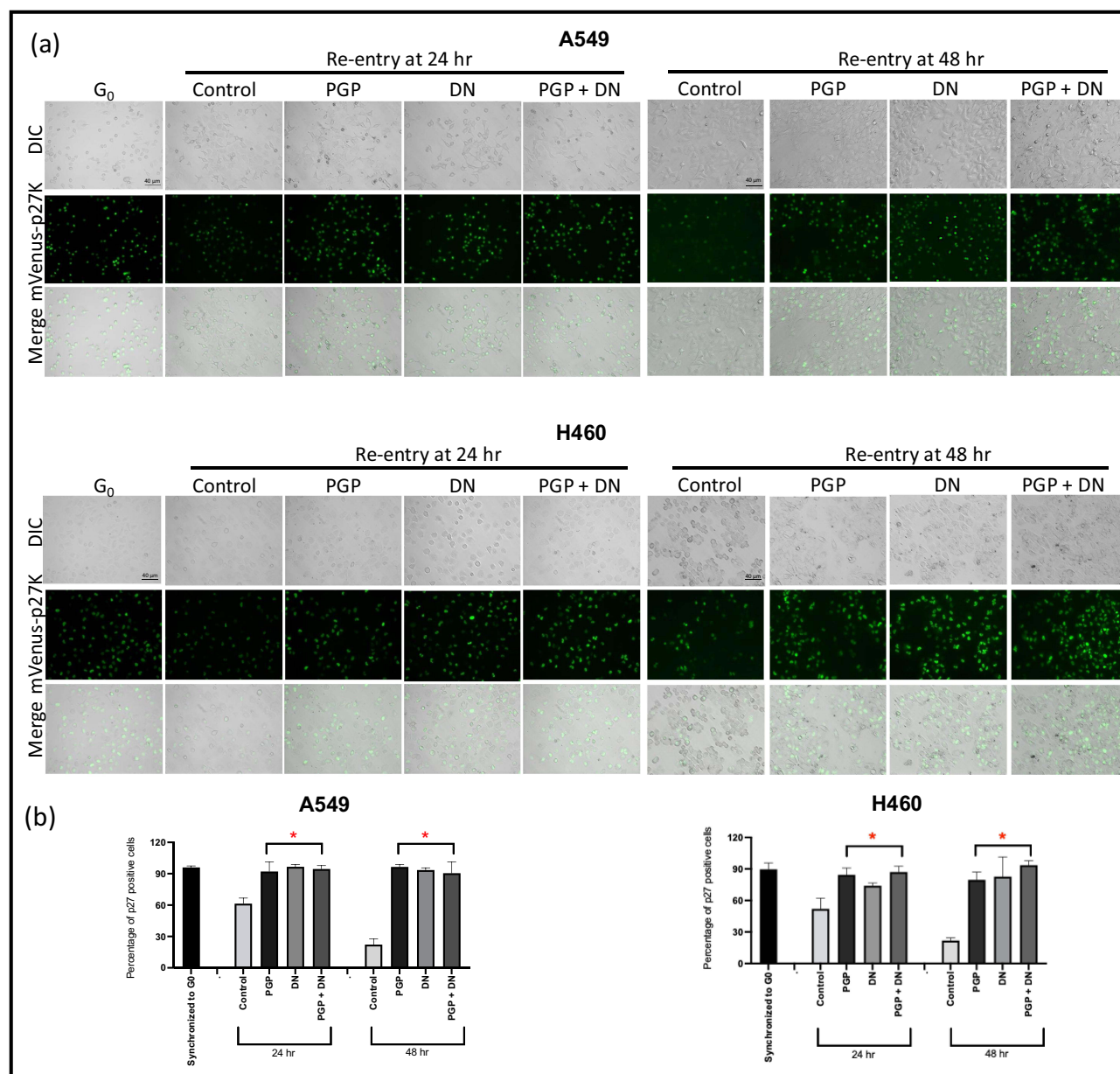


Figure 2 Retention of mVenus-p27K⁻ signal upon cell cycle reactivation by PGP, DN, and their combination. A549 and H460 cells with mVenus-p27K⁻ construct were enriched at G₀ state, and treatments were introduced once the cells were released from the dormant state. Cells were imaged after 24 h and 48 h of treatment. (a) Representative fluorescence images of G₀ cells, without or with treatments upon release from quiescence for A549 and H460 cells with the mVenus-p27K⁻ construct were presented. (b) The mVenus-p27K⁻ positive cells from the green fluorescence channel and the total number of cells from differential interference contrast (DIC) were counted using Image J. The percentage of mVenus-p27K⁻ positive cells from each sample was calculated from the ratio of green cells over the total number of cells. The average percentage from three biological replicates (n = 3) was presented. * indicates statistical significance compared with the control upon cell cycle re-entry (p < 0.05).

Chemical Profiling of PGP and DN

Ultra-High Performance Liquid Chromatography coupled with Quadrupole Time-of-Flight Mass Spectrometry (UPLC-Q-TOF/MS) analysis identified 24 phytochemicals in PGP and 23 in DN, including bioactive compounds with established anticancer properties. Novel compounds like fukiic acid (PGP; *m/z* 271.047) and polyphyllaside III (DN; *m/z* 1091.542) warrant further investigation for dormancy-specific roles.

PGP Profile ([Supplementary Table 3](#)): major constituents with high abundance (AUC > 4.6 million) include Punicalagin and ellagic acid,³² both known for inducing apoptosis and cell cycle arrest.^{11–15} Polyphenols including Gallic acid, brevifolincarboxylic acid, and corilagin were detected, corroborating PGP's antioxidant and antiproliferative activities.³²

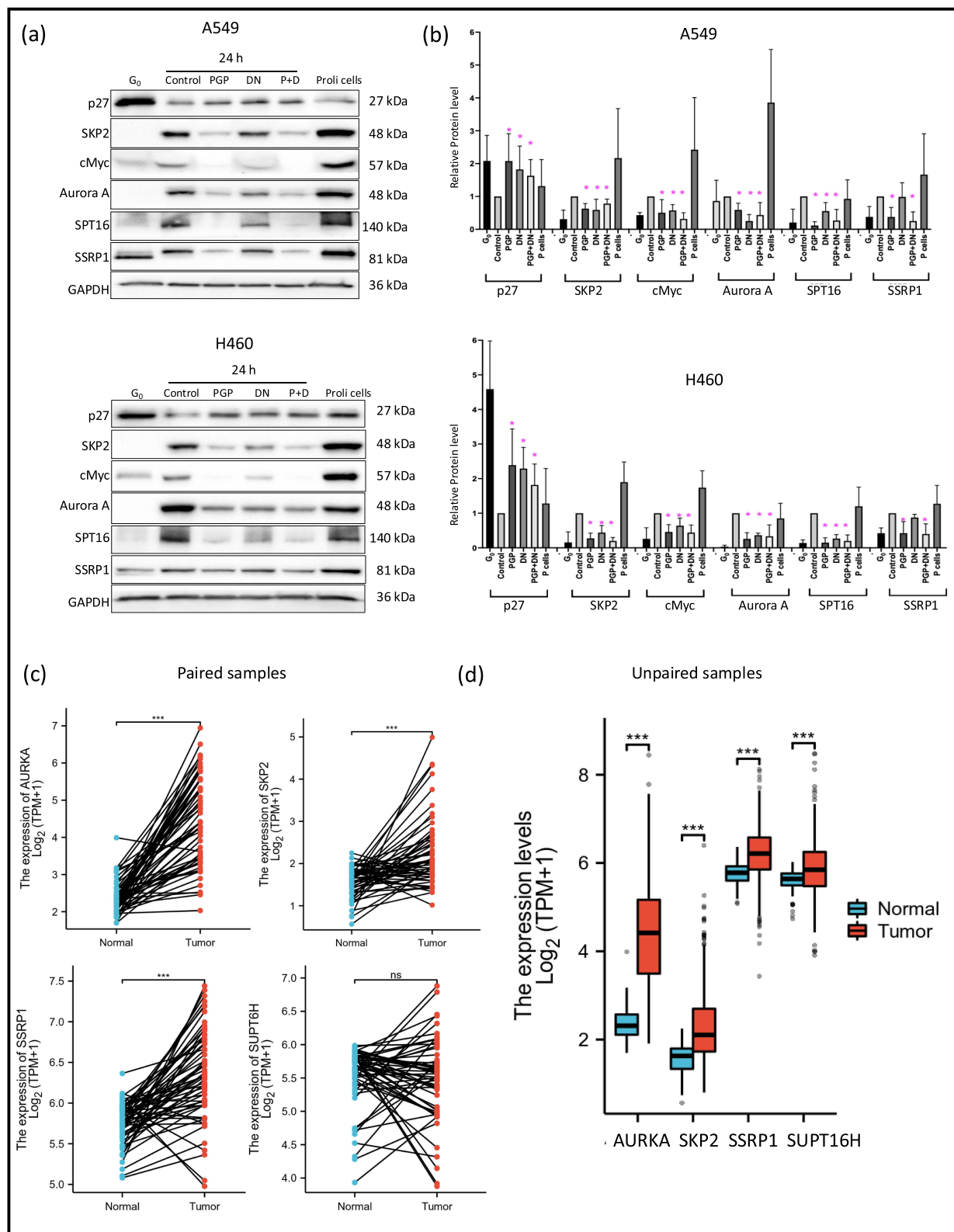


Figure 3 Modulation of key protein levels by treatments with PGP, DN, and their combination. (a) The treatments were introduced to lung cancer cells after releasing them from the dormant state and cells were harvested at 24 h for immunoblotting. (b) Quantification data of immunoblotting expressed as mean \pm SD ($n = 5$) of protein intensity determined by densitometry. Proliferative cells: Proliferative A549 and H460 cells' samples were used as control. * and *** indicate statistical significance compared with control ($p < 0.05$ and $p < 0.001$ respectively). The mRNA levels of cell cycle re-entry key regulators from 59 paired samples of lung adenocarcinoma and adjacent normal lung tissues (c), and unpaired 539 lung adenocarcinoma and 59 normal lung tissue samples (d) from TCGA database are presented.

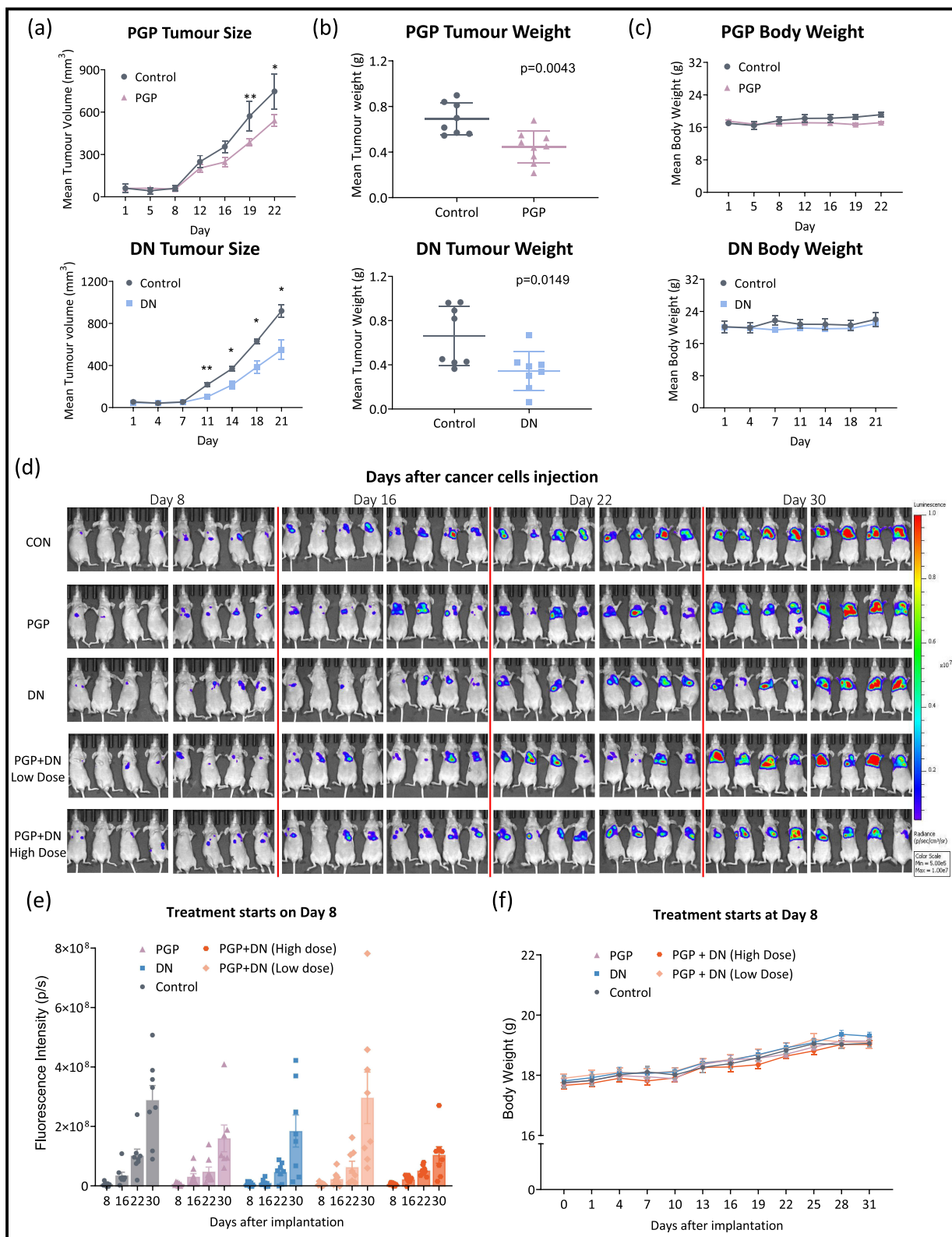


Figure 4 Impact of PGP, DN, and their combination on tumor metrics in xenograft and in situ models. (a) The effect of the PGP or DN treatment on tumour size and (b) weight and (c) body weight in xenograft animal model was assessed. Data expressed as mean \pm SEM ($n = 8$). (d) Bioluminescence images of the in situ animal model without or with treatments, (e) The fluorescence intensity of in situ tumours from Day 8 to Day 30, and (f) their body weight data are presented. Data expressed as mean \pm SEM ($n = 8$). * and ** indicate statistical significance compared with the control ($p < 0.05$ and $p < 0.01$ respectively).

DN Profile ([Supplementary Table 4](#)): Steroidal Saponins includes Dioscin and gracillin both showed significant abundance (AUC>4.7 million) and are potent inhibitors of MYC and SKP2 pathways.^{22,23} Saponin Derivatives including Protodioscin and pseudoprotogracillin were also identified, consistent with DN's reported role in ROS-mediated apoptosis.^{17,33,34} Fatty Acids and Triterpenoids including Tianshic acid and trillin highlighted DN's multi-target bioactivity.

Discussion

This study assessed the impact of *Punica granatum* peel (PGP) and *Dioscorea Nipponica* (DN) on dormant lung cancer cells, demonstrating that these agents not only inhibit DNA synthesis and cell cycle re-entry but also modulate key proteins involved in cell cycle regulation and dormancy maintenance. Notably, PGP and DN, either alone or in combination, effectively maintained the dormancy of lung cancer cells and significantly reduced tumor size and weight in xenograft models.

Dormant tumor cells, characterized by low proliferative and metabolic activity, play a crucial role in cancer recurrence and therapy resistance. These cells can evade therapeutic interventions and potentially reinitiate tumor growth under conducive internal and external conditions.^{5,35,36} Recent theories propose that a subpopulation of cancer stem cells, which remain dormant, could explain tumor persistence and relapse.^{6,37} Such cells are not only resistant to targeted therapies but can also self-renew and differentiate, thus contributing to treatment resistance. A pivotal study has linked these concepts by identifying a dormant p27⁺ subpopulation of cancer stem cells, indicating that conventional cancer drugs effectively target p27⁻ cancer stem cells but are ineffective against p27⁺ cells.³⁸ This integration of cancer dormancy and stem cell theories provides a critical foundation for our exploration of PGP and DN's effects on dormant lung cancer cells.

The therapeutic potential of this study is significant, particularly given the limited current clinical options like estrogen receptor modulators³⁹ and CDK4/6 inhibitors,⁴⁰ which primarily prevent tumor cells from exiting dormancy. Our findings suggest that PGP and DN offer a promising approach to targeting dormant tumor cells. The study showed that PGP and DN modulate a network of proteins critical for the transition from G₀ to G₁ phase. The proteins affected include p27, a key regulator of cell cycle dormancy, and SKP2, cMYC, AURORA A, and components of the FACT complex, all of which play significant roles in cell cycle progression and tumorigenesis.⁴¹ cMYC can suppress p27 transcription or indirectly reduce p27 protein stability via SKP2, part of the SCF^{SKP2} ubiquitin ligase complex, which is transcriptionally regulated by cMYC. The components of the FACT complex, SSRP1 and SUPT16H, are involved in promoting expression of p27 degradation protein including SKP2 and c-MYC.²⁵ AURORA A (AURKA) has been shown to form a complex with MYC preventing it from degradation. Moreover, by disrupting the MYC–AURKA complex, AURKA inhibitors stimulate MYC degradation and reduce tumor progression.^{42–44} Therefore, the decrease in SKP2, cMYC, AURKA, SUPT16H, and SSRP1, and stabilization of p27 in the presence of PGP and DN are likely to be responsible for hindering the G₀ to G₁ cell cycle transition and maintaining cells in a dormant state ([Figure 5](#)). While our data demonstrate that PGP and DN modulate MYC, SKP2, and p27 through upstream regulatory networks, further studies are required to determine whether specific compounds within these extracts directly bind to these targets or act via intermediary signaling cascades. The absence of sub-G₁ populations in treated cells, coupled with selective G₀ arrest and p27 stabilization, distinguishes the effects of PGP and DN from nonspecific cytotoxicity. These findings align with prior reports where dormancy regulators modulate cell cycle checkpoints without inducing cell death.⁴⁵ It is also important to note the functional stability of PGP and DN under simulated gastrointestinal conditions by SYBR Green assays, though metabolite profiling remains an avenue for future investigation.

The lack of overt synergy (Combination Index, CI<1) but observed additive efficacy (CI≈1) between PGP and DN at a 10:1 ratio offers insights into their mechanism of action and therapeutic potential. Synergy implies a cooperative interaction, often arising from complementary pathways. In contrast, additive effects reflect independent or overlapping mechanisms that cumulatively achieve the desired outcome without amplification. Both PGP and DN modulate overlapping dormancy regulators (p27 stabilization, SKP2/MYC suppression), suggesting their effects converge on the same pathways. While synergy is often idealized, additive effects in PGP-DN provide a pragmatic advantage for dormancy

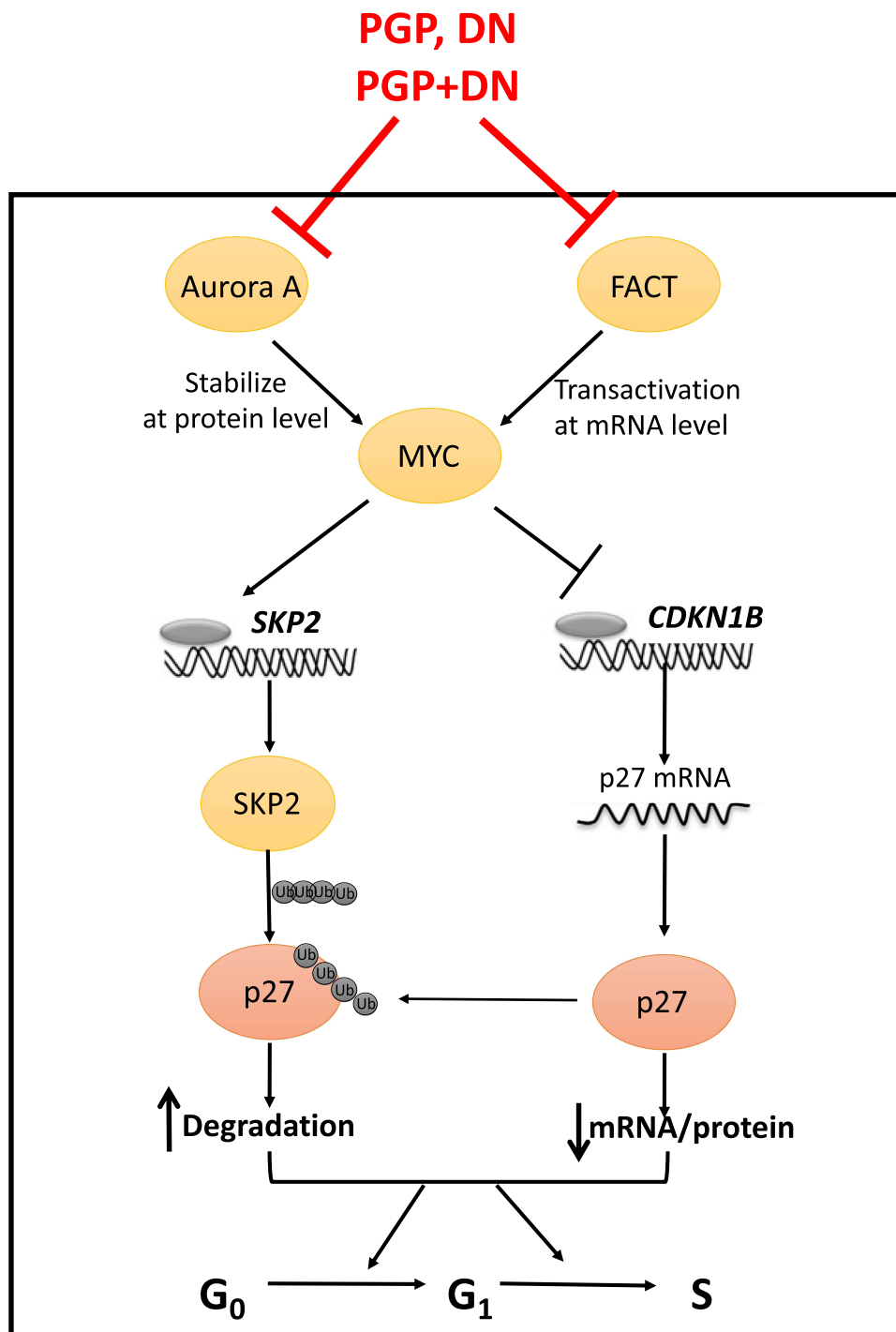


Figure 5 Biochemical pathways influenced by PGP, DN, and their combination in regulating cell cycle reactivation. Detailed pathways illustrate gene, mRNA, and protein interactions affecting cell cycle dynamics.

management, combining safety, multi-target coverage, and resistance prevention. This balance positions the combination as a viable candidate for translational development.

While PGP and DN show promise in preclinical models, clinical translation will require addressing bioavailability limitations, standardization challenges, and potential drug interactions. Future studies must prioritize pharmacokinetic profiling, long-term safety assessments, and compatibility with existing therapies to bridge these gaps. LC-MS/MS profiling

identified punicalagin and ellagic acid in PGP, and dioscin and gracillin in DN compounds with established anticancer activity in lung cancer. Punicalagin and ellagic acid disrupt MYC-driven proliferation and enhance chemosensitivity, while dioscin and gracillin induce apoptosis and inhibit metastatic signaling. These mechanisms in line with our observed dormancy-enforcing effects, positioning PGP and DN as multi-targeted agents against lung cancer recurrence. Further research should focus on identifying specific compounds within PGP and DN that impact dormancy-related pathways, offering novel insights into the action and mode of action. Although reductions in tumor volume in mouse models are indicative of efficacy, these models do not fully replicate the cell cycle re-entry dynamics of dormant cancer cells. Future studies should consider employing patient-derived tumor organoids and advanced in vivo imaging techniques to better understand the dynamics of dormancy and reactivation.

In conclusion, PGP and DN represent promising agents for sustaining lung cancer cell dormancy, potentially opening new avenues for preventing tumour recurrence. Our study enriches the understanding of how active components present in traditional Chinese Medicines can modulate key regulatory mechanisms in cancer biology, paving the way for novel therapeutic strategies against dormant tumour cells resistant to current treatments.

Abbreviations

AURKA, Aurora Kinase A gene; AURORA A, Aurora kinase A protein; BALB, Bagg Albino; CDKN1B, cyclin dependent kinase inhibitor 1B, which is also the name of gene coding for p27 protein; CI, Combination Index; CO₂, Carbon dioxide; DMSO, Dimethyl sulfoxide; DNA, Deoxyribonucleic acid; HBSS, Hank's Balanced Salt Solution; G₀, G₁ and S, different phases in cell cycle; mRNAs, messenger RNAs; MilliQ, Millipore Milli-Q; MYC, v-myc avian myelocytomatosis viral oncogene homolog; PBS, Phosphate-Buffered Saline; PVDF, Polyvinylidene fluoride; QLD, Queensland; RPMI, Roswell Park Memorial Institute; SDS-PAGE, Sodium dodecyl sulfate-polyacrylamide gel electrophoresis; SKP2, S-phase Kinase-associated Protein; SSRP1, Structure Specific Recognition Protein 1; SUPT16H, Suppressor of Ty Homolog-16; TCGA, The Cancer Genome Atlas.

Acknowledgments

The authors thank Dr Toshihiko Oki (The University of Tokyo, Tokyo, Japan) for the pMXs-IP-mVenus-p27K⁻ plasmid and Shanghai Laboratory Animal Research Center for conducting animal studies. The mRNA results from lung cancer specimens are based upon data generated by the TCGA Research Network: <https://www.cancer.gov/tcga>.

Author Contributions

All authors made a significant contribution to the work reported, whether that is in the conception, study design, execution, acquisition of data, analysis and interpretation, or in all these areas; took part in drafting, revising or critically reviewing the article; gave final approval of the version to be published; have agreed on the journal to which the article has been submitted; and agree to be accountable for all aspects of the work.

Funding

This study was sponsored by National Natural Science Foundation of China (82274143, 81904163) and Shanghai Oriental Talents Program (LB).

Disclosure

Chanlu Xie and Qihan Dong report a patent AU2021101338A issued. The authors declare no other competing interests.

References

1. Sung H, Ferlay J, Siegel RL, et al. Global cancer statistics 2020: GLOBOCAN estimates of incidence and mortality worldwide for 36 cancers in 185 countries. *CA Cancer J Clin.* 2021;71(3):209–249. doi:10.3322/caac.21660
2. Siegel RL, Miller KD, Fuchs HE, Jemal A. Cancer statistics, 2022. *CA Cancer J Clin.* 2022;72(1):7–33. doi:10.3322/caac.21708
3. Rotow JK, Lee JK, Madison RW, Oxnard GR, Janne PA, Schrock AB. Real-world genomic profile of EGFR second-site mutations and other osimertinib resistance mechanisms and clinical landscape of NSCLC post-osimertinib. *J Thorac Oncol.* 2024;19(2):227–239. doi:10.1016/j.jtho.2023.09.1453

4. Boyero L, Sanchez-Gastaldo A, Alonso M, Noguera-Ucles JF, Molina-Pinelo S, Bernabe-Caro R. Primary and acquired resistance to immunotherapy in lung cancer: unveiling the mechanisms underlying of immune checkpoint blockade therapy. *Cancers*. 2020;12(12):3729. doi:10.3390/cancers12123729
5. Phan TG, Croucher PI. The dormant cancer cell life cycle. *Nat Rev Cancer*. 2020;20(7):398–411. doi:10.1038/s41568-020-0263-0
6. Shen S, Vagner S, Robert C. Persistent cancer cells: the deadly survivors. *Cell*. 2020;183(4):860–874. doi:10.1016/j.cell.2020.10.027
7. Recasens A, Munoz L. Targeting cancer cell dormancy. *Trends Pharmacol Sci*. 2019;40(2):128–141. doi:10.1016/j.tips.2018.12.004
8. Saatci O, Huynh-Dam KT, Sahin O. Endocrine resistance in breast cancer: from molecular mechanisms to therapeutic strategies. *J Mol Med*. 2021;99(12):1691–1710. doi:10.1007/s00109-021-02136-5
9. Johnson N, Bentley J, Wang LZ, et al. Pre-clinical evaluation of cyclin-dependent kinase 2 and 1 inhibition in anti-estrogen-sensitive and resistant breast cancer cells. *Br J Cancer*. 2010;102(2):342–350. doi:10.1038/sj.bjc.6605479
10. Goel S, DeCristo MJ, McAllister SS, Zhao JJ. CDK4/6 inhibition in cancer: beyond cell cycle arrest. *Trends Cell Biol*. 2018;28(11):911–925. doi:10.1016/j.tcb.2018.07.002
11. Pan L, Yin D, Feixia M, Lou L. Punicalagin inhibits the viability, migration, invasion, and EMT by regulating GOLPH3 in breast cancer cells. *J Recept Signal Transduct*. 2020;40(2):173–180. doi:10.1080/10799893.2020.1719152
12. Ceci C, Lecal PM, Tentori L, De Martino MG, Miano R, Graziani G. Experimental evidence of the antitumor, antimetastatic and antiangiogenic activity of ellagic acid. *Nutrients*. 2018;10(11):1756. doi:10.3390/nu10111756
13. Adaramoye O, Erguen B, Nitzsche B, Höpfner M, Jung K, Rabien A. Punicalagin, a polyphenol from pomegranate fruit, induces growth inhibition and apoptosis in human PC-3 and LNCaP cells. *Chem Biol Interact*. 2017;274:100–106. doi:10.1016/j.cbi.2017.07.009
14. Hnit SST, Ding R, Bi L, et al. Agrimonia pilosa ledeb impedes cell cycle progression of cancer cells through G0 state arrest. *Biomed Pharmacother*. 2021;141:111795. doi:10.1016/j.biopha.2021.111795
15. Sun D-P, Huang H-Y, Chou C-L, et al. Punicalagin is cytotoxic to human colon cancer cells by modulating cell proliferation, apoptosis, and invasion. *Hum Exp Toxicol*. 2023;42:09603271231213979. doi:10.1177/09603271231213979
16. Faria A, Calhau C. The bioactivity of pomegranate: impact on health and disease. *Crit Rev Food Sci Nutr*. 2011;51(7):626–634. doi:10.1080/10408391003748100
17. Yao Y, Cui L, Ye J, et al. Dioscin facilitates ROS-induced apoptosis via the p38-MAPK/HSP27-mediated pathways in lung squamous cell carcinoma. *Int J Biol Sci*. 2020;16(15):2883–2894. doi:10.7150/ijbs.45710
18. Mao W, Yin H, Chen W, et al. Network pharmacology and experimental evidence reveal dioscin suppresses proliferation, invasion, and EMT via AKT/GSK3b/mTOR signaling in lung adenocarcinoma. *Drug Des Devel Ther*. 2020;14:2135–2147. doi:10.2147/dddt.S249651
19. Li Y, Liu H, Liu X, et al. Gracillin shows potential efficacy against non-small cell lung cancer through inhibiting the mtor pathway. *Front Oncol*. 2022;12:851300. doi:10.3389/fonc.2022.851300
20. Zhang G, Zeng X, Zhang R, et al. Dioscin suppresses hepatocellular carcinoma tumor growth by inducing apoptosis and regulation of TP53, BAX, BCL2 and cleaved CASP3. *Phytomedicine*. 2016;23(12):1329–1336. doi:10.1016/j.phymed.2016.07.003
21. Lim WC, Kim H, Kim YJ, et al. Dioscin suppresses TGF- β 1-induced epithelial-mesenchymal transition and suppresses A549 lung cancer migration and invasion. *Bioorg Med Chem Lett*. 2017;27(15):3342–3348. doi:10.1016/j.bmcl.2017.06.014
22. Wu Z, Han X, Tan G, et al. Dioscin inhibited glycolysis and induced cell apoptosis in colorectal cancer via promoting c-myc ubiquitination and subsequent hexokinase-2 suppression. *Onco Targets Ther*. 2020;13:31–44. doi:10.2147/ott.S224062
23. Zhou L, Yu X, Li M, et al. Cdh1-mediated skp2 degradation by dioscin reprogrammes aerobic glycolysis and inhibits colorectal cancer cells growth. *EBioMedicine*. 2020;51:102570. doi:10.1016/j.ebiom.2019.11.031
24. Oki T, Nishimura K, Kitaura J, et al. A novel cell-cycle-indicator, mVenus-p27K-, identifies quiescent cells and visualizes G0-G1 transition. *Sci Rep*. 2014;4(1):4012. doi:10.1038/srep04012
25. Bi L, Xie C, Yao M, et al. The histone chaperone complex FACT promotes proliferative switch of G0 cancer cells. *Int J Cancer*. 2019;145(1):164–178. doi:10.1002/ijc.32065
26. Bi L, Xie C, Jiao L, et al. CPF impedes cell cycle re-entry of quiescent lung cancer cells through transcriptional suppression of FACT and c-MYC. *J Cell Mol Med*. 2020;24(3):2229–2239. doi:10.1111/jcmm.14897
27. Yao M, Xie C, Constantine M, et al. How can food extracts consumed in the Mediterranean and East Asia suppress prostate cancer proliferation? *Br J Nutr*. 2012;108(3):424–430. doi:10.1017/S0007114511005770
28. Bermu'dez-Soto MJ, Toma's-Barbera'n FA, Garc'a-Conesa MT. Stability of polyphenols in chokeberry (*Aronia melanocarpa*) subjected to in vitro gastric and pancreatic digestion. *Food Chem*. 2007;102(3):865–874. doi:10.1016/j.foodchem.2006.06.025
29. Commission TSP. *Pharmacopoeia of the P.R. China*. Beijing: Chemical Industry Press; 2010.
30. Chernick MR. *Bootstrap Methods: A Guide for Practitioners and Researchers*. Wiley; 2008.
31. Shapiro HM. Flow cytometric estimation of DNA and RNA content in intact cells stained with Hoechst 33342 and pyronin Y. *Cytometry*. 1981;2(3):143–150. doi:10.1002/cyto.990020302
32. Fischer UA, Carle R, Kammerer DR. Identification and quantification of phenolic compounds from pomegranate (*Punica granatum L.*) peel, mesocarp, aril and differently produced juices by HPLC-DAD-ESI/MSn. *Food Chem*. 2011;127(2):807–821. doi:10.1016/j.foodchem.2010.12.156
33. Chen H, Wang L, Wang C, et al. Strategy of combining offline 2D LC-MS with LC-DIA-MS/MS to accurately identify chemical compounds and for quality control of *Dioscorea septemloba* Thunb. *Phytochem Anal*. 2022;33(7):1135–1146. doi:10.1002/pca.3165
34. Lin CL, Lee CH, Chen CM, et al. Protodioscin induces apoptosis through ROS-mediated endoplasmic reticulum stress via the JNK/p38 activation pathways in human cervical cancer cells. *Cell Physiol Biochem*. 2018;46(1):322–334. doi:10.1159/000488433
35. Kreso A, O'Brien CA, van Galen P, et al. Variable clonal repopulation dynamics influence chemotherapy response in colorectal cancer. *Science*. 2013;339(6119):5438. doi:10.1126/science.1227670
36. Giancotti FG. Mechanisms governing metastatic dormancy and reactivation. *Cell*. 2013;155(4):750–764. doi:10.1016/j.cell.2013.10.029
37. Nassar D, Blanpain C. Cancer stem cells: basic concepts and therapeutic implications. *Annu Rev Pathol*. 2016;11(1):47–76. doi:10.1146/annurev-pathol-012615-044438
38. Ohta Y, Fujii M, Takahashi S, et al. Cell-matrix interface regulates dormancy in human colon cancer stem cells. *Nature*. 2022;608(7924):784–794. doi:10.1038/s41586-022-05043-y

39. Xu Y, Huangyang P, Wang Y, et al. ERalpha is an RNA-binding protein sustaining tumor cell survival and drug resistance. *Cell*. 2021;184(20):5215–5229e17. doi:10.1016/j.cell.2021.08.036
40. O’Leary B, Finn RS, Turner NC. Treating cancer with selective CDK4/6 inhibitors. *Nat Rev Clin Oncol*. 2016;13(7):417–430. doi:10.1038/nrclinonc.2016.26
41. Nik Nabil WN, Xi Z, Song Z, et al. Towards a framework for better understanding of quiescent cancer cells. *Cells*. 2021;10(3):562. doi:10.3390/cells10030562
42. Brockmann M, Poon E, Berry T, et al. Small molecule inhibitors of aurora-a induce proteasomal degradation of N-myc in childhood neuroblastoma. *Cancer Cell*. 2013;24(1):75–89. doi:10.1016/j.ccr.2013.05.005
43. Richards MW, Burgess SG, Poon E, et al. Structural basis of N-Myc binding by aurora-A and its destabilization by kinase inhibitors. *Proc Natl Acad Sci U S A*. 2016;113(48):13726–13731. doi:10.1073/pnas.1610626113
44. Doha ZO, Sears RC. Unraveling MYC’s role in orchestrating tumor intrinsic and tumor microenvironment interactions driving tumorigenesis and drug resistance. *Pathophysiology*. 2023;30(3):400–419. doi:10.3390/pathophysiology30030031
45. Drexler HCA, Pebler S. Inducible p27Kip1 expression inhibits proliferation of K562 cells and protects against apoptosis induction by proteasome inhibitors. *Cell Death Differ*. 2003;10(3):290–301. doi:10.1038/sj.cdd.4401159

Drug Design, Development and Therapy

Dovepress
Taylor & Francis Group

Publish your work in this journal

Drug Design, Development and Therapy is an international, peer-reviewed open-access journal that spans the spectrum of drug design and development through to clinical applications. Clinical outcomes, patient safety, and programs for the development and effective, safe, and sustained use of medicines are a feature of the journal, which has also been accepted for indexing on PubMed Central. The manuscript management system is completely online and includes a very quick and fair peer-review system, which is all easy to use. Visit <http://www.dovepress.com/testimonials.php> to read real quotes from published authors.

Submit your manuscript here: <https://www.dovepress.com/drug-design-development-and-therapy-journal>